New Approach for Predicting Flow Bifurcation at Right-Angled Open-Channel Junction

G. Kesserwani[1]; J. Vazquez[2]; N. Rivière[3]; Q. Liang[4]; G. Travin[5]; and R. Mosé[6]

Abstract: An unsteady mathematical model for predicting flow divisions at a right-angled open-channel junction is presented. Existing dividing models depend on a prior knowledge of a constant flow regime. In addition, their strong nonlinearity does not guarantee compatibility with the St. Venant solutions in the context of an internal boundary condition treatment. Assuming zero crest height at the junction region, a side weir model explicitly introduced within the one-dimensional St. Venant equations is used to cope with the two-dimensional pattern of the flow. An upwind implicit numerical solver is employed to compute the new governing equations. The performance of the proposed technique in predicting super-, trans-, and subcritical flow bifurcations is illustrated by comparing with experimental data and/or theoretical predictions. In all the tests, lateral-to-upstream discharge ratios (R_q) are successfully reproduced by the present technique with a maximum error magnitude of less than 9%.

DOI: 10.1061/(ASCE)HY.1943-7900.0000222

CE Database subject headings: Weirs; Open channel flow; Flow numerical models; Bifurcations; Comparative studies; Predictions.

Author keywords: *T*-junction; Side weir; Open channels; Flow division; Numerical modeling; 1D; St. Venant; Comparisons.

Introduction

Flow separation through a right-angled open-channel network, or a *T*-junction, is commonly encountered within many water engineering applications. This kind of flow is mainly characterized by inflow and outflow discharges, upstream and downstream water depths, and a lateral outflow. Detailed hydrodynamics of *T*-junction flows are found to be complex and strongly three dimensional (3D) in the vicinity of the junction (e.g., Ramamurthy et al. 2007). However, in some industrial designs in hydraulic and environmental engineering, a one-dimensional (1D) approach could be practically and economically attractive and the scientific issue may be treated by simplified hypotheses.

Earliest literature on open-channel junction flows was presented by Taylor (1944) showing that the number of equations provided by a 1D analysis based on the conservation of momentum is incomplete to analytically solve the junction problem (Kesserwani et al. 2008a,b). Rajaratnam and Pattabiramiah (1960) regarded the branch channel problem as a lateral overflow through a side weir of zero sill height. Law and Reynolds (1966) examined the dividing *T*-junction flow at a low Froude number (F), using the momentum and the energy principles. When focusing on the subcritical flow regime, Ramamurthy and Satish (1988) theoretically and experimentally investigated dividing flows with an unsubmerged lateral branch. The investigators developed a theoretical model relating the downstream-to-upstream depth (h_d/h_u) and discharge (Q_d/Q_u) ratios with the upstream Froude number (F_u). A more general expression was later formulated by Ramamurthy et al. (1990) with no restriction on the flow nature at the lateral branch. Hsu et al. (2002) established a depth-discharge relationship and an energy-loss coefficient derived from the energy equation. Rivière et al. (2006) studied the influence of a second inlet. For subcritical flow divisions, the best that can be expected is an approximate theoretical relationship linking Q_d/Q_u and h_d/h_u. For the transcritical regime—subcritical regime with a transition to the supercritical regime in the lateral branch—approximate relationships to predict flow distribution at a *T*-junction may be obtained as function of F_u and/or F_d where the subscript d refers to a downstream quantity (Krishnappa and Seetharamiah 1963; Lakshmana-Rao and Sridharan 1967; Ramamurthy and Satish 1988; Rivière et al. 2007). Generally the use of such relationships requires an independent estimate of h at some points. Finally, in the supercritical regime, Sridhran and Rao (1966) analyzed the flow division at low F in a *T*-junction assuming a constant specific energy along a side weir. The discharge in the lateral branch can be computed by the formula derived by Mizumura et al. (2003) for overflowing supercritical rivers, which compares well with experiments.

Common to these relationships, their implementation requires a prior knowledge of the flow regime, which is not obvious to be determined without making additional assumptions. Moreover, during a storm event, flooding may have a transient behavior with

[1]Research Associate, School of Civil Engineering and Geosciences, Newcastle Univ., Newcastle upon Tyne NE1 7RU, U.K. (corresponding author). E-mail: georges.kesserwani@ncl.ac.uk

[2]Lecturer, ENGEES-IMFS, Univ. de Strasbourg, 4 rue Boussingault, 67000 Strasbourg, France. E-mail: jvazquez@engees.u-strasbg.fr

[3]Professor, LMFA, Univ. de Lyon, CNRS-ECL-INSAL-UCBL1, INSA de Lyon, 20 Ave. A. Einstein, 69621 Villeurbanne, France. E-mail: riviere@insa-lyon.fr

[4]Lecturer, School of Civil Engineering and Geosciences, Newcastle Univ., Newcastle upon Tyne NE1 7RU, U.K. E-mail: qiuhua.liang@newcastle.ac.uk

[5]Assistant Professor, LMFA, Univ. de Lyon, CNRS-ECL-INSAL-UCBL1, INSA de Lyon, 20 Ave. A. Einstein, 69621 Villeurbanne, France. E-mail: gilbert.travin@insa-lyon.fr

[6]Professor, ENGEES-IMFS, Univ. de Strasbourg, 4 rue Boussingault, 67000 Strasbourg, France. E-mail: rmose@engees.u-strasbg.fr

Note. This manuscript was submitted on July 20, 2008; approved on March 10, 2010; published online on March 12, 2010. Discussion period open until February 1, 2011; separate discussions must be submitted for individual papers. This technical note is part of the ***Journal of Hydraulic Engineering***, Vol. 136, No. 9, September 1, 2010. ©ASCE, ISSN 0733-9429/2010/9-662–668/$25.00.

a changing flow regime from sub- to supercritical, or vice versa. In such circumstance, it is difficult to ensure constant flow regime and thus approximate relationships become inappropriate. On the other hand, a 1D numerical approach with an internal boundary condition treatment (Kesserwani et al. 2008a,b) accommodated by a theoretical dividing model (e.g., Ramamurthy et al. 1990; Hsu et al. 2002) may fall short because a nonlinear system has to be solved, at each time step, and this does not always ensure the convergence of the solutions.

In the light of Rajaratnam and Pattabiramiah (1960), the current work examines an alternative to predict flow bifurcation at a T-junction. A modified form to the St. Venant equations is proposed to model lateral outflow effects. Applying an upwind numerical scheme, the solutions to the modified unsteady model are used to determine the discharge ratio of the lateral outflow to the main inflow. The relationships developed by Mizumura et al. (2003), Rivière et al. (2007), and experimental data (Hsu et al. 2002; Rivière et al. 2007) are used to validate the present approach for super-, trans-, and subcritical flow bifurcations.

Mathematical Model and Numerical Scheme

Mathematical Model

For an inflow divided into two parts, side and downstream, the lateral portion is modeled with the side weir model of Hager (1987). The side weir model with a zero crest height at the intersection area is coupled with a conservative form of the 1D St. Venant equations. From mass and momentum conservation principles across a control volume including a continuous lateral outflow, the 1D system of equations modeling unsteady flow in a channel of variable width and depth can be expressed in the following vectorial conservative form

$$\mathbf{U}_t + \mathbf{F}_x = \mathbf{S} \tag{1}$$

in which t represents the time (s) and x represents the longitudinal distance (m); $\mathbf{U}$=vector of the conserved quantities, or the flow variables; $\mathbf{F}$=flux vector; and $\mathbf{S}$=vector containing the source terms and the effect of a lateral diversion. They are given by

$$\mathbf{U} = \begin{pmatrix} A \\ Q \end{pmatrix}, \quad \mathbf{F} = \begin{pmatrix} Q \\ \dfrac{Q^2}{A} + gI_1 \end{pmatrix}$$

$$\text{and} \quad \mathbf{S} = \begin{pmatrix} Q_L \\ gA(S_0 - S_f) + gI_2 + \dfrac{QQ_L}{A} \end{pmatrix} \tag{2}$$

where g=acceleration due to gravity ($\mathrm{m/s^2}$); $A(x,t)$=cross-sectional wetted area ($\mathrm{m^2}$); $Q(x,t)$=discharge ($\mathrm{m^3/s}$); I_1 and I_2=integral terms accounting, respectively, for the hydrostatic pressure forces and the pressure forces caused by the variation of the channel along the main stream direction; $S_0=-\partial z/\partial x$ designates the bed slope defined as the derivative of the ground elevation $z(x)$; and S_f denotes the friction slope modeled with the Manning empirical law $S_f=n_M^2u^2/R_h^{4/3}$, where R_h=hydraulic radius; $u=Q/A$=mean velocity; and n_M ($\mathrm{s/m^{1/3}}$)=roughness coefficient.

The Jacobian ($\mathbf{J}=\partial\mathbf{F}/\partial\mathbf{U}$) of the flux vector with respect to the flow vector has two real eigenvalues $\lambda^{1,2}=u\pm c$ and two associated real eigenvectors $\mathbf{e}^{1,2}=[1,\lambda^{1,2}]^T$, where $c=(gA/B)^{1/2}$=wave celerity speed (B=channel width at the free surface).

Hager's (1987) side weir model for the discharge per unit length (Q_L) is

$$Q_L = -\frac{3}{5}c_{0L}\sqrt{gH^3}(y-W)^{3/2}\left(\frac{1-W}{3-2y-W}\right)^{1/2} \times\left[1-(\theta_{0L}+S_{0L})\left(\frac{3-3y}{y-W}\right)^{1/2}\right] \tag{3}$$

where $y=h/H$ and $W=w/H$=dimensionless water depth and side crest height, respectively, and H=energy head expressed in terms of h (m). θ_{0L} and S_{0L}=contraction angle (=0 for the present study) and slope of the side weir. The coefficient c_{0L} model the weir-crest influence ($c_{0L}=1$ for a thin wall).

Numerical Scheme

Since no transient propagations of flow discontinuities are considered in the following applications, the upwind Roe (1981) scheme with implicit time integration is practical and sufficient for the current study (Kesserwani et al. 2007). For completeness, the adopted numerical scheme is briefly outlined.

The spatial domain is discretized by (x_i,t_n), where $x_i=i\Delta x$; $i=1,2,\ldots,N$ and $t_n=n\Delta t$; $n=1,2,\ldots$; Δt=time; Δx=uniform grid spacing; and N=number of computational cells. By respectively denoting the approximate vectors $\mathbf{U}(x_i,t_n)$, $\mathbf{F}(x_i,t_n)$, and $\mathbf{S}(x_i,t_n)$ by $\mathbf{U}_i^n$, $\mathbf{F}_i^n$, and $\mathbf{S}_i^n$ and performing algebraic manipulations, a general implicit discretized form of Eq. (1) is obtained as follows

$$\mathbf{U}_i^{n+1} + \frac{\Delta t}{\Delta x}(\tilde{\mathbf{F}}_{i+1/2}^{n+1} - \tilde{\mathbf{F}}_{i-1/2}^{n+1}) - \Delta t\mathbf{S}_i^{n+1} = \mathbf{U}_i^n \tag{4}$$

The implicit operator is linearized following the methodology of Yee (1987) such that a conservative linearized form of Eq. (4) is obtained and a tridiagonal system has to be solved

$$\mathbf{A}_i^1\delta\mathbf{U}_{i-1} + \mathbf{A}_i^2\delta\mathbf{U}_i + \mathbf{A}_i^3\delta\mathbf{U}_{i+1} = \mathbf{A}_i^4 \tag{5}$$

where $\delta\mathbf{U}_i=\mathbf{U}_i^{n+1}-\mathbf{U}_i^n$. The local coefficients $\mathbf{A}_i^{1,2,3}$ are 2×2 matrices and $\mathbf{A}_i^4$ is the traditional Godunov-type discrete operator having the following structures

$$\mathbf{A}_i^{1,3} = \mp\frac{\Delta t}{2\Delta x}(\mathbf{J}_{i\mp1}^n \pm \mathbf{M}_{i\mp1/2}^n)$$

$$\mathbf{A}_i^2 = \mathbf{I} + \frac{\Delta t}{2\Delta x}(\mathbf{M}_{i+1/2}^n + \mathbf{M}_{i-1/2}^n) - \Delta t\mathbf{J}_\mathbf{S}$$

$$\mathbf{A}_i^4 = -\frac{\Delta t}{2\Delta x}(\tilde{\mathbf{F}}_{i+1/2}^n - \tilde{\mathbf{F}}_{i-1/2}^n) + \Delta t\mathbf{S}_i^n \tag{6}$$

where $\mathbf{I}$=identity matrix and $\mathbf{M}_{i\pm1/2}^n$ reads

$$\mathbf{M}_{i\pm1/2} = \frac{1}{\tilde{\lambda}_{i\pm1/2}^2 - \tilde{\lambda}_{i\pm1/2}^1} \times\begin{pmatrix} d_{i\pm1/2}^1\tilde{\lambda}_{i\pm1/2}^2 - d_{i\pm1/2}^2\tilde{\lambda}_{i\pm1/2}^1 & d_{i\pm1/2}^2 - d_{i\pm1/2}^1 \\ \tilde{\lambda}_{i\pm1/2}^1\tilde{\lambda}_{i\pm1/2}^2(d_{i\pm1/2}^1 - d_{i\pm1/2}^2) & d_{i\pm1/2}^2\tilde{\lambda}_{i\pm1/2}^2 - d_{i\pm1/2}^1\tilde{\lambda}_{i\pm1/2}^1 \end{pmatrix} \tag{7}$$

In Eqs. (6) and (7), $\mathbf{J}_\mathbf{S}$ denotes the Jacobian matrix of the source vector with respect to the flow vector (García-Navarro et al. 1994); $\tilde{\mathbf{F}}_{i\pm1/2}^n$ are, respectively, the fluxes across the interfaces $x_{i\pm1/2}$ estimated by the Riemann solver of Roe (1981). The terms $d_{i+1/2}^{1,2}$ are given by

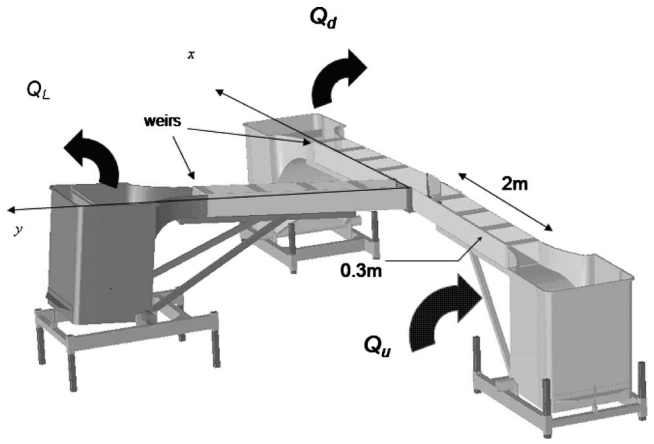

Fig. 1. Schematic layout of the experimental facility available at the INSA of Lyon

$$d_{i+1/2}^{1,2} = -\psi(\tilde{\lambda}_{i+1/2}^{1,2})\alpha_{i+1/2}^{1,2} \tag{8}$$

$\tilde{\lambda}_{i+1/2}^{1,2}$ and the wave strengths $\alpha_{i+1/2}^{1,2}$ can be expressed by means of the Roe averaged velocity and celerity (Roe 1981) and Ψ is the entropy fix function of Harten and Hyman (1983). The source term components in Eq. (2) are discretized by using the upwind philosophy of Bermúdez and Vázquez (1994).

Numerical Results and Discussions

Theoretical models (Mizumura et al. 2003; Rivière et al. 2007) and/or experimental data (Hsu et al. 2002; Rivière et al. 2007) are used to assess the performance of the modified 1D St. Venant model to predict flow divisions at a *T*-junction. At the computational level, a main reach, linking the upstream and downstream channels, is presumed whereas the lateral branch is treated as a

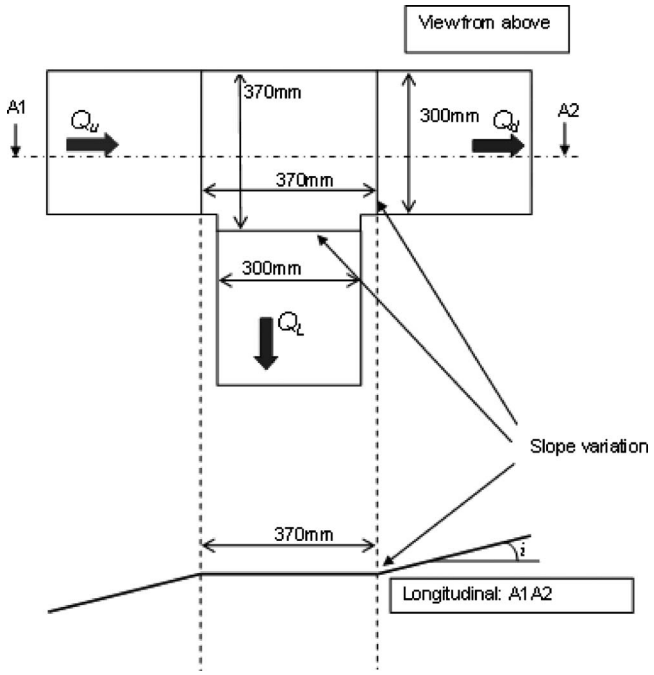

Fig. 2. Experimental setup viewed from above

Table 1. Supercritical Flow Bifurcations: Inflow Conditions; Computational (Comp.); and Theoretical R_q and Corresponding Error [Eq. (13)]

Reach slope (%)	$Q_u \times 10^3$ (m^3/s)	$h_u \times 10^2$ (m)	F_u	R_q (comp.) (%)	R_q [Eq. (10)] (%)	Error [Eq. (13)] (%)
1	2.0	1.2	1.70	20.7	16.3	−4.40
1	3.0	1.5	1.76	19.6	15.8	−3.80
1	4.0	1.8	1.81	18.9	15.5	−3.40
1	5.0	2.0	1.85	18.5	15.2	−3.30
1	6.0	2.3	1.88	18.2	14.9	−3.30
1	6.9	2.5	1.90	17.8	14.8	−3.00
1	8.1	2.7	1.93	17.5	14.6	−2.90
1	9.1	2.9	1.95	17.3	14.5	−2.80
1	10.0	3.1	1.97	17.1	14.3	−2.80
1	11.0	3.3	1.98	17.0	14.3	−2.70
1	12.0	3.4	2.00	16.9	14.1	−2.80
3	3.5	1.1	3.17	11.4	9.1	−2.30
3	4.0	1.2	3.21	11.2	9.0	−2.20
3	4.5	1.3	3.25	11.0	8.9	−2.10
3	5.0	1.4	3.28	10.9	8.8	−2.10
3	5.5	1.5	3.31	10.7	8.8	−1.90
3	6.0	1.5	3.34	10.6	8.7	−1.90
3	6.5	1.6	3.37	10.5	8.6	−1.90
3	7.0	1.7	3.40	10.4	8.6	−1.80
3	7.5	1.8	3.42	10.3	8.5	−1.80
3	8.0	1.8	3.44	10.2	8.4	−1.80
3	8.5	1.9	3.46	10.1	8.4	−1.70
3	9.0	2.0	3.48	10.0	8.4	−1.60
3	9.5	2.0	3.50	10.0	8.3	−1.70
5.75	10.7	1.9	4.19	8.2	7.0	−1.20
5.75	8.5	1.6	4.34	8.0	6.7	−1.30
5.75	9.1	1.7	4.38	7.9	6.7	−1.20
5.75	4.0	1.0	4.50	8.1	6.5	−1.60
5.75	10.5	1.8	4.57	7.6	6.4	−1.20
5.75	10.1	1.8	4.59	7.6	6.4	−1.20
5.75	5.0	1.1	4.60	7.8	6.3	−1.50
5.75	6.5	1.3	4.73	7.5	6.2	−1.30
5.75	7.0	1.4	4.77	7.5	6.1	−1.40
5.75	7.5	1.4	4.80	7.4	6.1	−1.30
5.75	8.1	1.5	4.84	7.3	6.0	−1.30
5.75	9.6	1.6	4.92	7.2	5.9	−1.30

side weir overflow. A grid of $N=201$ computational points is considered for the computations with a refinement of $N/3$ at the zone covered by the side weir (i.e., at the intersection). The Courant-Friedrich-Levy (CFL) number is chosen equal to 5 (Kesserwani et al. 2007). By default, the dimensions of the computational reach and Manning's factor are selected in conformity with the below described experimental apparatus. After attaining a stationary state with respect to a given inflow and/or outflow steady condition, the outflow numerical discharge is recorded (Q_d). Assuming mass continuity at the junction, the lateral diversion can be obtained by the difference between the inflow and the outflow discharges ($Q_L=Q_u-Q_d$), and the associated lateral-to-upstream discharge ratio (R_q) writes

$$R_q = \frac{Q_L}{Q_u} \tag{9}$$

where the subscripts u, L, and d, respectively, indicate the flow

Table 2. Transcritical Flow Bifurcations: Inflow Discharges and Outflow Frontal Weir Conditions; Experimental (Exp.), Computational (Comp.), and Theoretical R_q Values; Error [Eq. (13)] Evaluated with Reference to the Experimental and the Theoretical Observations

$w_d \times 10^3$ (m)	$Q_u \times 10^3$ (m^3/s)	F_d	F_u	R_q (exp.) (%)	R_q (comp.) (%)	R_q [Eq. (14)] (%)	Error (exp.) (%)	Error [Eq. (14)] (%)
99.6	15.06	0.01	0.49	97.5	100.0	97.6	−2.5	−2.4
85.3	12.04	0.02	0.49	95.2	100.0	95.5	−4.8	−4.5
99.6	16.02	0.03	0.50	94.3	98.2	93.4	−4.0	−4.8
75	10.92	0.03	0.50	92.7	97.7	93.4	−5.0	−4.3
99.6	17.03	0.04	0.51	91.1	97.0	91.3	−5.9	−5.7
99.6	18.02	0.05	0.52	89.5	95.8	89.3	−6.3	−6.5
85.3	14.03	0.05	0.53	89.8	95.6	89.3	−5.8	−6.3
99.6	19.03	0.06	0.54	87.2	94.2	87.3	−7.0	−6.9
99.6	19.99	0.07	0.55	85.8	92.6	85.4	−6.8	−7.2
75	13.00	0.07	0.55	85.8	92.4	85.4	−6.6	−7.0
85.3	16.03	0.08	0.55	84.9	91.7	83.6	−6.7	−8.1
85.3	18.03	0.10	0.57	81.1	88.5	80.0	−7.3	−8.5
85.3	20.11	0.10	0.58	78.8	83.8	80.0	−5.0	−3.8
75	15.08	0.11	0.59	80.5	87.3	78.3	−6.8	−9.0
50	10.00	0.13	0.62	74.4	77.8	74.9	−3.4	−2.9
75	17.00	0.14	0.63	76.5	82.3	73.3	−5.8	−9.0
50	12.00	0.17	0.67	68.7	70.5	68.7	−1.8	−1.8
50	14.00	0.20	0.71	64.9	64.4	64.4	0.5	0.0
40	10.59	0.23	0.72	62.4	61.8	60.3	0.7	−1.5
50	15.60	0.24	0.76	60.8	60.7	59.1	0.1	−1.6
40	13.30	0.28	0.81	56.1	53.5	54.2	2.6	0.7
40	14.98	0.30	0.82	53.3	50.9	51.9	2.3	1.0
40	19.00	0.34	0.90	48.0	44.7	47.7	3.3	3.0
40	17.00	0.35	0.92	49.2	47.7	46.7	1.5	−1.0

parameters corresponding to the upstream, lateral, and downstream branches. The results are illustrated in a number of tables listing the predicted R_q versus reference ones together with their corresponding inflow and/or outflow conditions.

Overview of the Experimental Setup

Experimental data were gathered in the channel intersection facility located at the Laboratory of Fluid Mechanics and Acoustics in Lyon, France (Mignot et al. 2008). Data are available for sub- and transcritical flow bifurcation cases (Rivière et al. 2007). The facility consisted of four glass channels, 0.3 m wide and 2 m long, with independently varying slopes. By blocking the inflow contribution from the lateral channel at the crossroad area, the network system was reduced to three (rectangular) open channels, as depicted in Fig. 1. The intersection is $0.3 \times 0.3\ m^2$ but it is mounted on a $0.37 \times 0.37\ m^2$ base with a zero slope (see Fig. 2). In this setup, one reach provided the main inflow and two others operated as outflow channels. The inflow reach was supplied from a large storage tank at the upstream end, where a honeycomb serves to stabilize and straighten the inlet flow. The inflow discharge Q_u could be set independently from 0.002 to 0.02 m^3/s. After ensuring stationary conditions, all inflow and outflow discharges were measured (one depth, respectively, upstream and downstream of the junction) by electromagnetic sensors with a measurement uncertainty of $5 \times 10^{-5}\ m^3/s$. Corresponding water depth based Reynolds numbers range from 2.7×10^3 to 2.7×10^4. With glass walls, the flow is hydraulically smooth, leading to equivalent Manning's roughness coefficients in the range ($0.0077\ s/m^{-1/3}$; $0.0091\ s/m^{-1/3}$). The mean value of $n_M = 0.0083\ s/m^{-1/3}$ is considered in the sequel. In the subcritical and transcritical bifurcation cases, all channels were horizontal. Due to the moderate values of the Reynolds number, a calibrated weir equation was used to provide a downstream condition $h_k(k=L,d)$ as a function of w_k, Q_k, and B_k (Rivière et al. 2007), where $w_k(k=L,d)$ represents the heights of the weirs located at the edges of the lateral and downstream branches (Fig. 1), respectively. When $w_k > 0 (k=L,d)$, the weirs are submerged in order to ensure a subcritical flow during the whole experiment. Selecting $w_k=0$ removed the submerged status for the weirs leading to a free outflow downstream condition.

Evaluation of the Proposed Technique

Supercritical Bifurcation

The supercritical flow regime is maintained in this case at the inflow and outflows. Identical sloping bed configurations are used for the upstream and downstream (computational) branches and for side weir model (3). Three subsets of cases are accordingly considered associated with bed slopes of 1, 3, and 5.75%, respectively. Physical inflow conditions are furnished to the numerical solver and the outflow information is completed by numerical boundary conditions. The set of inflow conditions, consisting of the depth h_u and discharge Q_u, is available in Table 1 whereby $1.70 \leq F_u \leq 4.92$. Table 1 also includes the predicted R_q values compared with those calculated via the theoretical relationship of Mizumura et al. (2003). Given F_u, the theoretical R_q is determined as (independently from the channel's characteristics being used)

Table 3. Subcritical Flow Bifurcations ($w_L=w_d$): Inflow Discharges and Outflow Frontal Weir Conditions; Computational (Comp.) and Experimental (Exp.) R_q and Their Deviation [Eq. (13)]

$w_d\times10^3$ (m)	$Q_u\times10^3$ (m^3/s)	F_d	R_q (exp.) (%)	R_q (comp.) (%)	Error (exp.) (%)
120.4	2.02	0.02197	47.8	49.7	−1.9
120.4	2.984	0.03054	49.3	49.3	0.1
80	2.006	0.03911	48.8	49.1	−0.3
120.4	5.023	0.04732	49.2	49.0	0.2
80	3.009	0.05292	49.0	48.8	0.2
60	1.99	0.05575	48.7	48.7	0.0
120.4	8.013	0.06942	49.0	48.5	0.5
60	3.04	0.07821	47.8	48.2	−0.4
80	5.067	0.08232	47.6	48.2	−0.6
40	2.003	0.0933	48.2	48.7	−0.5
120.4	11.94	0.09355	48.7	48.0	0.7
60	5.037	0.11265	47.6	47.3	0.3
80	8.05	0.113	47.5	47.4	0.2
40	3.028	0.12688	46.5	46.9	−0.4
80	11.975	0.15012	46.7	46.3	0.5
60	8.02	0.15741	46.6	45.9	0.6
40	5.07	0.1789	46.0	45.1	0.8
80	15.04	0.17312	46.4	45.5	1.0
20.1	2.01	0.19876	46.0	44.8	1.2
60	12.06	0.20401	45.2	44.3	1.0
80	18.986	0.20178	44.9	44.7	0.2
40	8	0.23926	44.0	42.9	1.1
60	15.11	0.23376	43.9	43.2	0.8
20.1	3.008	0.25776	43.6	42.5	1.0
60	19.08	0.26704	42.6	41.8	0.8
40	12	0.3002	41.8	40.3	1.5
20.1	5.016	0.34246	41.1	38.8	2.4
40	14.98	0.33626	40.0	38.6	1.4
10	1.997	0.37424	39.6	39.3	0.2
40	18.96	0.37475	38.0	36.2	1.8
20.1	7.987	0.42783	36.1	32.7	3.4
10	2.991	0.45812	35.6	33.9	1.8
20.1	9.66	0.46282	33.9	28.8	5.1
10	4.004	0.51286	32.5	29.5	3.0

$$R_q = \frac{1}{F_u}\left[\frac{\cos^3(\beta+\theta/\sqrt{3})}{\cos^3(\theta/\sqrt{3})}\right] \tag{10}$$

where β and θ are related to F_u by

$$\cos\left(\frac{\theta}{\sqrt{3}}\right) = \sqrt{\frac{3}{2+F_u^2}} \tag{11}$$

and

$$\sin(\beta) = \frac{1}{F_u} \tag{12}$$

A quantitative evaluation can be achieved by calculating the deviation of each predicted ratio from the reference ratio via the error consisting of their difference

$$\text{error} = R_q(\text{reference}) - R_q(\text{computed}) \tag{13}$$

Taking the theoretical predictions as a reference, the produced error, which is adjoined in Table 1, is found to be always negative and, decreasingly, varying between −4.4 and −1.3% with the average of −2.11%. The theoretical predictions of Eq. (10) for the experiments of Mizumura et al. (2003) have been also found larger than the measured data with decreasing difference (13) in proportion to an increasing F_u (Mizumura 2005). The relative error, obtained by Eq. (13) divided by R_q reference, remains comparatively unaffected.

Transcritical Bifurcation

In this test, subcritical flow is considered at the upstream and downstream reaches ($w_d>0$) while the lateral branch is unsubmerged ($w_L=0$) leading to a transcritical flow bifurcation. The upstream inflow (Q_u) is specified as a physical boundary condition. Outflow boundary conditions are completed by a weir stage-discharge condition (Rivière et al. 2007). Several cases are defined and simulated according to Q_u and w_d available in Table 2, whereby $0.01\leqslant F_d\leqslant 0.35$. Applying the relationship of Ramamurthy et al. (1990), the associated F_u is found bounded by $0.49\leqslant F_u\leqslant 0.92$. Error (13), with reference to the experimental data, varied between −7.3 and +3.3% with predominantly negative values forming a mean error of −3.4%. Table 2 further displays the predictions carried out by the empirical model of Rivière et al. (2007), which is a correction of the model of Lakshmana-Rao and Sridharan (1967). For a specified F_d, the theoretical R_q reads

$$\log_{10}(R_q) + 0.925F_d^{0.98} = 0 \tag{14}$$

A bigger averaged error, equal to −4.0%, is acquired with regard to the theoretical predictions ranging between −9 and 3%. Compared to the errors produced relating to the experiments, this error is in some cases larger and in some others smaller with a tiny discrepancy. Globally, the numerical predictions compare favorably the theoretical calculations and the experimental data.

Subcritical Bifurcation

The same configurations to those used in the previous test are made for the upstream and downstream floodways. However, the frontal weir placed at the downstream end of the lateral branch is also in a submerged state ($w_L>0$) to obtained a wholly subcritical flow through the T-junction system. A case can be defined by means of Q_u and the two weir lengths $w_{L,d}$ (see Tables 3 and 4). Within the computational model, Q_u is specified while h_d is obtained by a calibrated frontal weir condition (Rivière et al. 2007). Additionally, the diverted outflow must be passed under submerged conditions (Tullis et al. 2007). Therefore, Q_L is amended using Villemonte's (1947) relationship

$$Q_L^* = Q_L\left[1-\left(\frac{H}{H_L}\right)^{1.5}\right]^{0.385} \tag{15}$$

where H_L=the head downstream of the side weir (expressed in terms of h_L). The considered cases are classified into two categories depending on either the two frontal weirs are identical or of different crest heights. Table 3 contains the cases of which the outflow conditions are identical ($w_L=w_d$) while Table 4 summarizes the cases obtained by different outflow settings ($w_L\neq w_d$). In both tables, weir heights, inflow discharges, and experimental and computed R_q values are listed together with generated error (13). F_d varied between 0.015 and 0.51. An estimate of F_u can be obtained via the equation of Ramamurthy et al. (1990) ($0.04\leqslant F_u\leqslant 0.85$). Very good numerical predictions are achieved compared with the experimental data. With an averaged

Table 4. Subcritical Flow Bifurcations ($w_L \neq w_d$): Inflow Discharges and Outflow Frontal Weir Conditions; Computational (Comp.) and Experimental (Exp.) R_q and Their Deviation [Eq. (13)]

$w_L \times 10^3$ (m)	$w_d \times 10^3$ (m)	$Q_u \times 10^3$ (m^3/s)	F_d	R_q (exp.) (%)	R_q (comp.) (%)	Error (exp.) (%)
30.06	45	20	0.1215	42.5	42.5	0.0
35	45	20	0.12785	40.8	41.5	−0.7
39.97	45	19.97	0.13537	38.9	39.8	−0.9
45	45	19.98	0.14433	36.7	37.9	−1.2
55.07	45	19.96	0.16274	32.7	33.7	−1.1
75.13	45	19.95	0.21063	24.2	24.3	−0.1
95.3	45	20	0.28651	15.1	14.8	0.2
20.02	49.3	6	0.01649	78.7	77.8	0.8
25	49.3	6.031	0.02118	73.8	73.4	0.4
29.93	49.3	5.99	0.0261	68.4	68.7	−0.3
40	49.3	5.988	0.03741	56.9	57.5	−0.6
49.4	49.3	5.98	0.05066	46.3	45.7	0.6
60	49.3	6.027	0.06858	34.0	31.8	2.2
70.2	49.3	6.008	0.08985	22.8	19.0	3.8
85.1	49.3	6.009	0.13367	6.8	3.9	2.9
16.01	19.9	5.989	0.13129	42.1	39.4	2.7
18.1	19.9	5.98	0.13751	40.6	38.2	2.4
20.07	19.9	5.98	0.14447	38.8	36.8	2.0
25.1	19.9	6.02	0.16573	34.1	32.6	1.5
30.14	19.9	5.998	0.19274	29.1	27.5	1.6
40.04	19.9	6	0.25397	20.1	17.0	3.1
50.04	19.9	6.003	0.35164	10.9	7.1	3.8
55	19.9	5.99	0.44145	5.8	2.9	2.9
12.17	35.2	6.01	0.03546	68.2	64.9	3.3
15.06	35.2	6.016	0.04011	64.9	63.0	1.9
20.3	35.2	6.003	0.04827	60.0	58.7	1.2
30.12	35.2	6.005	0.06474	49.5	49.1	0.4
35.12	35.2	6.012	0.07549	44.1	43.4	0.7
15	35.2	10.07	0.07193	55.1	51.4	3.7
18.1	35.2	10.05	0.07628	53.4	50.0	3.4
24.2	35.2	10.058	0.08528	49.8	47.0	2.9
30.15	35.2	10.046	0.09566	46.2	43.4	2.8
35.2	35.2	10.04	0.10591	42.5	40.1	2.5
12.6	60.2	9.976	0.01509	82.2	78.2	4.0
19.2	60.2	9.98	0.01942	77.7	74.9	2.7
30.16	60.2	9.98	0.02667	70.5	68.6	1.9
32	60.2	9.99	0.02809	68.6	67.2	1.3
45	60.2	9.96	0.03955	59.2	58.0	1.3
60.2	60.2	9.99	0.05697	46.8	45.1	1.7

error of +1.2%, the model tended to slightly overestimate the measured data with random altering between −1.9 and 5.1%. Some additional cases from literature have been simulated consistent with the experimental resource of Hsu et al. (2002). As displayed in Table 5, satisfactory results are also achieved with an averaged error of +1.27%.

Summary and Conclusions

A new approach was proposed for predicting flow divisions at a *T*-junction. The method was used for the calculation of discharge ratios of a side outflow to the main channel flow. The lateral outflow, described by Hager's (1987) side weir model, was explicitly integrated within the source terms of the unsteady open-channel flow equations. The numerical solution to the modified St. Venant model was implemented using an upwind implicit scheme allowing a numerical prediction of lateral-to-upstream discharge ratio (R_q). No calibration parameters were set to the proposed technique. The numerical outcomes were first evaluated in supercritical flow regime and compared to theoretical calculations. The predictions are quite accurate, although the numerical calculations are found to be always (fairly) larger than the theoretical ones. In transcritical flow conditions, the numerical results are comparable to the reference ratios and the error switched to positive for inflow Froude numbers greater than 0.7. These observations could be expected as with the two latter regimes, the side weir was unsubmerged and hence the branch flow was not influenced by any downstream condition. In subcritical regime, the accuracy of the numerical results is more surprising; the use of a submerged weir equation was able to account for the downstream control in the side branch. As a whole, the numerical predictions agree closely with the experimental data or those provided by empirical formulas, with, respectively, an absolute value to the averaged and maximum errors not exceeding 4 and 9%.

Table 5. Subcritical Flow Bifurcations (Hsu et al. 2002): Inflow Discharges and Outflow Depth Conditions; Computational (Comp.) and Experimental (Exp.) R_q and Their Deviation [Eq. (13)]

$Q_u \times 10^3$ (m^3/s)	$h_d \times 10^2$ (m)	F_d	R_q (exp.) (%)	R_q (comp.) (%)	Error (exp.) (%)
4.57	8.53	0.25	39.6	36.7	2.8
5.06	8.9	0.26	38.7	37.7	0.9
3.02	4.91	0.53	12.9	15.56	−2.6
3.05	4.79	0.53	17.3	9.5	7.8
3.92	5.77	0.54	12.5	11.22	1.2
3.54	5.14	0.56	16.6	15.2	1.4

Notation

The following symbols are used in this technical note:

A = wetted area;
B = width at the free surface;
c = wave celerity;
c_{0L} = weir-crest influence;
$\mathbf{e}^{1,2}$ = eigenvector associated with $\lambda^{1,2}$;
$\mathbf{F}$ = flux vector;
$\tilde{\mathbf{F}}$ = two argument numerical flux function;
F = Froude number;
g = gravitational forces;
H = total energy;
h = water depth;
I_1 = hydrostatic pressure term;
I_2 = wall pressure term;
$\mathbf{J}$ = Jacobian of $\mathbf{F}$ with respect to $\mathbf{U}$;
$\mathbf{J_s}$ = Jacobian of $\mathbf{S}$ with respect to $\mathbf{U}$;
N = number of computational points;
n = time step;
n_M = roughness coefficient;
Q = flow discharge;
Q^* = flow rate over a submerged weir;
R_h = hydraulic radius;
$R_q = Q_L/Q_d$ = lateral-to-upstream discharge ratio;

$\mathbf{S}$ = source term vector;
S_0 = bed slope;
S_{0L} = bottom slope of the side weir;
S_f = friction term;
t = time;
$\mathbf{U}$ = vector of the flow variables;
u = averaged velocity;
w = weir height;
W = dimensionless variable of the weir height;
x = longitudinal distance;
y = dimensionless variable of the water depth;
z = ground elevation;
$\alpha^{1,2}$ = wave strengths;
Δt = time increment;
Δx = grid space;
θ_{0L} = contraction angle of the side weir;
$\lambda^{1,2}$ = eigenvalues of the Jacobian $\mathbf{J}$; and
ψ = entropy fix function.

Subscripts

d = downstream of the main channel;
L = upstream of the lateral channel; and
u = upstream of the main channel.

References

Bermúdez, A., and Vázquez, M. E. (1994). "Upwind methods for hyperbolic conservation laws with source terms." *Comput. Fluids*, 23(8), 1049–1071.

García-Navarro, P., Alcrudo, F., and Priestley, A. (1994). "An implicit method for water flow modelling in channels and pipes." *J. Hydraul. Res.*, 32(5), 721–742.

Hager, W. H. (1987). "Lateral outflow over side weirs." *J. Hydraul. Eng.*, 113(4), 491–504.

Harten, A., and Hyman, J. M. (1983). "Self adjusting grid methods for one-dimensional hyperbolic conservation laws." *J. Comput. Phys.*, 50(2), 235–269.

Hsu, C. C., Tang, C. J., Lee, W. J., and Shieh, M. Y. (2002). "Subcritical 90° equal-width open-channel dividing flow." *J. Hydraul. Eng.*, 128(7), 716–720.

Kesserwani, G., Ghostine, R., Vazquez, J., Ghenaim, A., and Mosé, R. (2008b). "One-dimensional simulation of supercritical flow at a confluence by means of a nonlinear junction model applied with the RKDG2 method." *Int. J. Numer. Methods Fluids*, 57(12), 1695–1708.

Kesserwani, G., Ghostine, R., Vazquez, J., Mosé, R., Abdallah, M., and Ghenaim, A. (2008a). "Simulation of subcritical flow at open-channel junction." *Adv. Water Resour.*, 31(2), 287–297.

Kesserwani, G., Ghostine, R., Vazquez, J., Mosé, R., and Ghenaim, A. (2007). "Simulation unidimensionnelle de l'écoulement à surface libre avec un schema numérique TVD en discrétisation implicite et explicite." *Houille Blanche*, 5, 101–106.

Krishnappa, G., and Seetharamiah, J. (1963). "A new method for predicting the flow at a 90° branch channel." *Houille Blanche*, 7, 775–778.

Lakshmana-Rao, N. S., and Sridharan, K. (1967). "Division of flow in open channels." *Irrig. Power*, 24(4), 393–407.

Law, S. W., and Reynolds, A. J. (1966). "Dividing flow in an open channel." *J. Hydr. Div.*, 92(2), 207–231.

Mignot, E., Rivière, N., Perkins, R., and Paquier, A. (2008). "Flow patterns in a four-branch junction with supercritical flow." *J. Hydraul. Eng.*, 134(6), 701–713.

Mizumura, K. (2005). "Discharge ratio of side outflow to supercritical channel flow." *J. Hydraul. Eng.*, 131(9), 821–824.

Mizumura, K., Yamasaka, M., and Adachi, J. (2003). "Side outflow from supercritical channel flow." *J. Hydraul. Eng.*, 129(10), 769–774.

Rajaratnam, N., and Pattabiramiah, K. R. (1960). "A new method to predict flow in a branch channel." *Irrig. Power*.

Ramamurthy, A. S., Qu, J., and Vo, D. (2007). "Numerical and experimental study of dividing open-channel flows." *J. Hydraul. Eng.*, 133(10), 1135–1144.

Ramamurthy, A. S., and Satish, M. G. (1988). "Division of flow in short open channel branches." *J. Hydraul. Eng.*, 114(4), 428–438.

Ramamurthy, A. S., Tran, D. M., and Carballada, B. L. (1990). "Dividing flow in open channels." *J. Hydraul. Eng.*, 116(3), 449–456.

Rivière, N., Perkins, R. J., Chocat, B., and Lecus, A. (2006). "Flooding flows in city crossroads: 1D modelling and prediction." *Water Sci. Technol.*, 54(6–7), 75–82 (IWA).

Rivière, N., Travin, G., and Perkins, R. J. (2007). "Transcritical flows in open channel intersections." *Proc., 32nd IAHR Congress* (CD-ROM), Venice, Italy, IAHR, Paper SS05–11.

Roe, P. L. (1981). "Approximate Riemann solvers, parameter vectors, and difference schemes." *J. Comput. Phys.*, 43(2), 357–372.

Sridhran, K., and Rao, N. S. L. (1966). "A new solution to division of flow in open channels." *J. Inst. Eng. (India), Part AG*, 48(3), 123–140.

Taylor, E. H. (1944). "Flow characteristics at rectangular open-channel junctions." *ASCE Trans*, 109, 893–912.

Tullis, B. P., Young, J. C., and Chandler, M. A. (2007). "Head-discharge relationships for submerged labyrinth weirs." *J. Hydraul. Eng.*, 133(3), 248–254.

Villemonte, J. (1947). "Submerged-weir discharge studies." *Eng. News-Rec.*, 139(26), 54–56.

Yee, H. C. (1987). "Construction of explicit and implicit symmetric TVD schemes and their applications." *J. Comput. Phys.*, 68(1), 151–179.